Available online at http://www.journalcra.com

International Journal of Current Research
Vol. 7, Issue, 12, pp.23584-23591, December, 2015

INTERNATIONAL JOURNAL OF CURRENT RESEARCH

ISSN: 0975-833X

RESEARCH ARTICLE

STRUCTURE AND DIELECTRIC PROPERTIES OF SOL GEL PROCESSED Ba (Fe1/2Nb1/2) O3 CERAMICS

[1]Krimech, F., [*,1]Sayouri, S. , [2]Zouhairi, M., [2]El ghadraoui, El. and [3]Elbasset, A.

[1]Laboratory of Theoretical and Applied Physics, FSDM, B. P. 1796, Fes Atlas, Morocco
[2]Laboratory of Chemistry of Condensed Matter, FST, B. P. 2202, Fes, Morocco
[3]Laboratory of Signals, Systems and Components, FST, B. P. 2202, Fes, Morocco

ARTICLE INFO

Article History:
Received 25th September, 2015
Received in revised form
17th October, 2015
Accepted 19th November, 2015
Published online 21st December, 2015

Key words:

Perovskite,
Sol Gel, BFN,
Dielectric properties.

ABSTRACT

In this work, barium iron niobate, Ba (Fe1/2Nb1/2) O3 powder has been successfully synthesized by the sol-gel method. The formation of the perovskite structure of BFN was followed with the help of X-ray diffraction (XRD), and has shown a crystallite size at a nanometric scale. The pure perovskite phase was obtained at relatively low temperature (900°C /8 h) compared to the conventional solid-state reaction. Moreover, dielectric measurements showed strong relaxation and diffuse phenomena, and a maximum of the dielectric permittivity at a temperature lower than those reported in the literature, together with resonance phenomenon at high frequency values. Impedance parameters were extracted from the permittivity analysis and enabled us in particular, to determine the coefficient charge of the sample.

***Citation*:** Krimech, F., Sayouri, S,. Zouhairi, M., El ghadraoui, El. and Elbasset, A., 2015. "Structure and dielectric properties of sol gel processed Ba (Fe1/2Nb1/2) O3 ceramics", *International Journal of Current Research*, 7, (12), 23584-23591.

INTRODUCTION

Due to its interesting dielectric properties, much attention has been devoted to the study of barium iron niobate Ba $(Fe_{1/2}Nb_{1/2})$ O_3 (BFN). Indeed, it has been reported that this material is a ferroelectric relaxor possessing a high dielectric permittivity (Eitssayeam *et al*., 2006; Homes *et al*., 2003; Raevski *et al*., 2003; Saha and Sinha, 2002 a,b; Tezuka *et al*., 2000; Subramanian *et al*., 2000; Yokosuka, 1995) with a broad and frequency dependent maximum at a temperature around 170°C (Saha and Sinha, 2002 a,b).BFN belongs to the family of complex perovskites such as Pb $(Mg_{1/3}Nb_{2/3})$ O_3 and $CaCu_3Ti_4O_{12}$ that are very good candidates for electromechanic applications. This material has been synthesized with different methods: co-precipitation (Nipaphat and Rakchart, 2011), solid state reaction (Ganguly *et al*., 2011, Saha and Sinha, 2002 b), sol gel method (Chao-Yu Chung *et al*., 2005), molten salt route (Nattaya *et al*., 2012); However, concerning its structure, it has been reported that BFN may adopt either the cubic structure or the monoclinic one (Rama *et al*., 2004; Saha and Sinha, 2002b). In the present study, the BFN compound has been prepared by the sol gel process.

Corresponding author: Sayouri, S.
Laboratory of Theoretical and Applied Physics, FSDM, B. P. 1796, Fes Atlas, Morocco.

The choice of this method of processing was based on its various advantages in comparison to other ones, namely, low processing temperature, high purity, homogeneity and an excellent control of the stoichiometry of the products (Limame *et al*., 2008). We have investigated the structure and microstructure of the samples using X-ray diffraction (XRD) and scanning electron microscopy (SEM). We have also performed dielectric measurements for frequencies ranging from 500 Hz to 2 MHz, and for temperatures such as 30 < T< 300 °C.

MATERIALS AND METHODS

The Ba $(Fe_{1/2}Nb_{1/2})$ O_3 powders were prepared by a sol-gel process using barium chloride $[BaCl_2{\cdot}2H_2O]$, iron chloride $[FeCl_3{\cdot}6H_2O]$, niobium chloride $[NbCl_5]$ and citric acid anhydrous. The purities of all the chemicals were over 99.9%. The flow chart of the experimental procedure is given in Fig.1. The citric acid, iron chloride and barium chloride were dissolved in distilled water while the niobium chloride was dissolved in ethanol. All the solutions were thoroughly mixed in an ambient atmosphere using a magnetic stirrer. The precursors containing Ba, Fe and Nb were dried in an oven at 120°C for 10 h.

The samples were subsequently calcined at various temperatures from 600°C to 900°C for 8 hours. The progress of the reaction was followed with the help of an X-ray diffractometer (XRD) with CuKα (λ=1.5405Å) radiation. For dielectric measurements, the powder samples were pressed into pellets with a uniaxial pressure of 8 tons/cm^2, and then sintered at 1100°C for 8 h, with a heating rate of 5°C/min. The microstructure of the ceramics was examined by scanning electron microscopy (SEM) (Quanta 200 FEI model EDAX).

RESULTS AND DISCUSSION

X-ray diffraction study

Fig.2 shows the X-ray diffraction patterns obtained on the BFN powders calcined at different temperatures from 600°C to 900°C for 8 hours. A beginning of the crystallization is observed for 600 °C and 700°C.

The spectrum of the sample calcined at 850°C shows the main peaks of the perovskite structure (BFN). The formation of the BFN perovskite phase seems complete, without the presence of secondary phases; when the samples were calcined at the temperature of 900°C during 8h. The duration, 8h, of the calcination step was chosen because it gave a well resolved pattern. Indeed, Fig.3 gives the X-ray diffraction patterns obtained on the BFN powders calcined at 900°C for different times (5h, 8h and 12h). The crystallization of BFN in the perovskite structure is observed when the duration, t, of the calcinations step is 5h with a considerable amount of residual phases. The crystallization in the pure perovskite phase is achieved when t is equal to 8 h, while a further increase in the calcination time, t= 12h, affects drastically the powder structure. All the diffraction peaks of the XRD pattern (Fig.3) can be indexed according to a monoclinic structure. Since the early 1960s, BFN has been known as a cubic perovskite with the lattice parameter a = 0.4045 nm (Raevski *et al*., 1996).

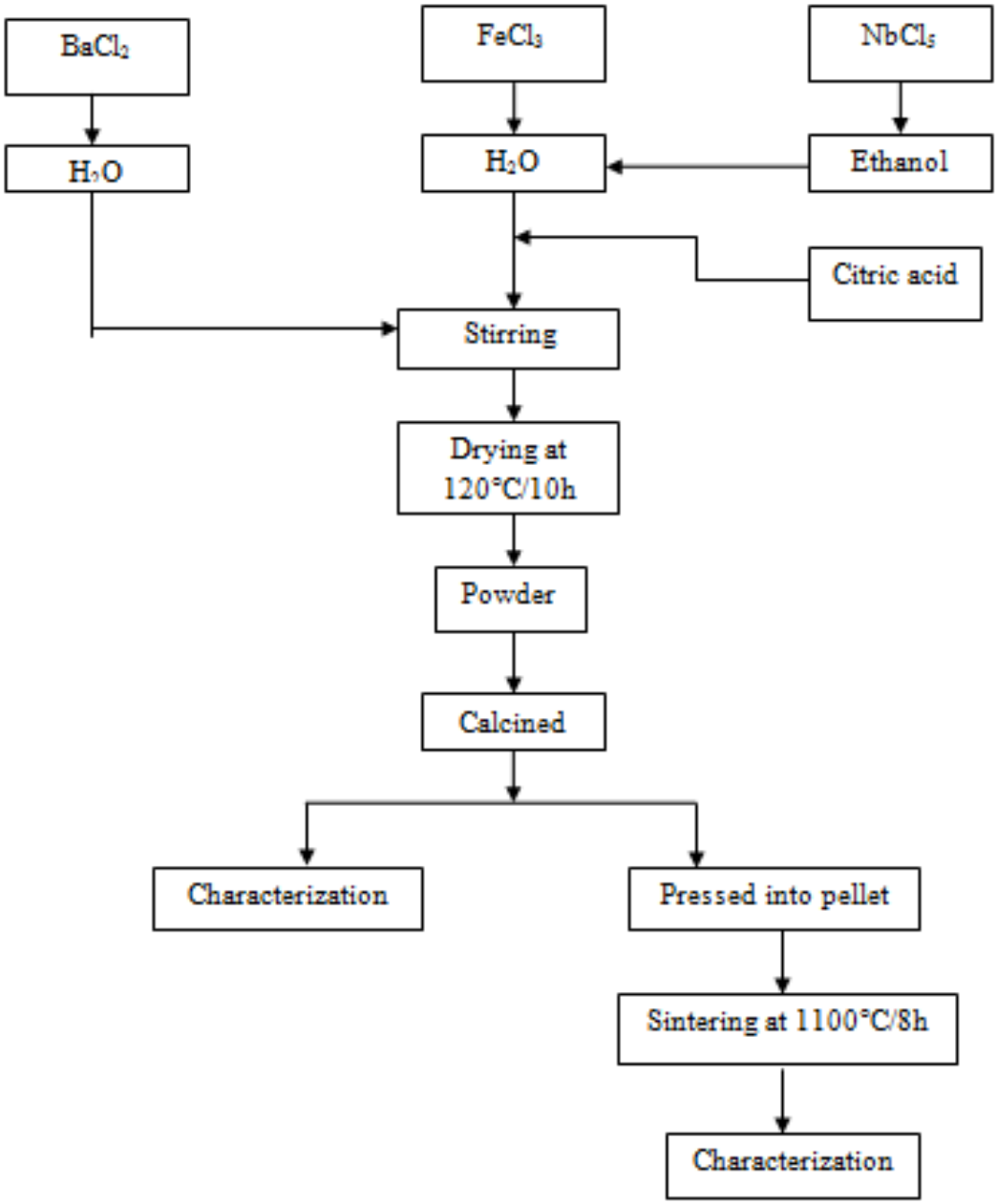

Fig. 1. Illustration of the preparation of the BFN powders and BFN ceramic by sol-gel method

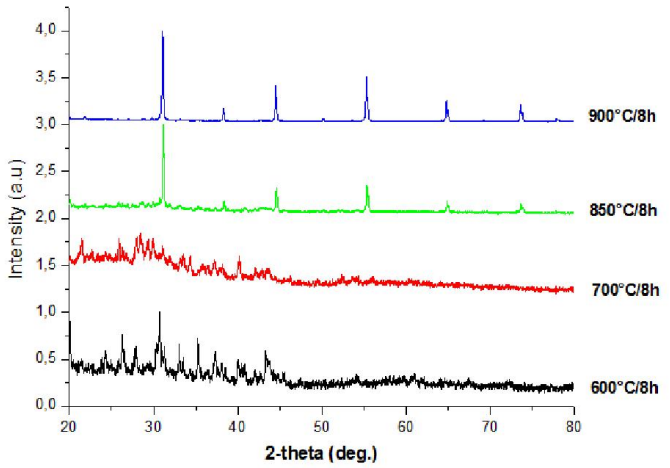

Fig. 2. XRD patterns of heat-treated BFN powders

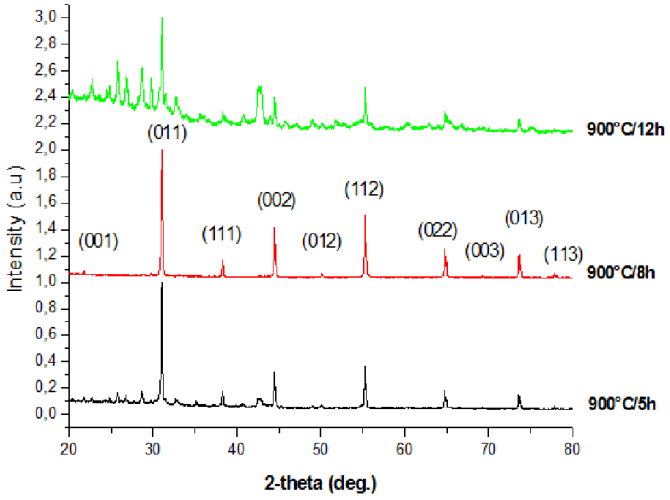

Fig. 3. XRD patterns of the BFN powders calcined at 900° C for various times

Our XRD analysis has revealed a pure monoclinic phase, without the presence of secondary phases, with the following parameters: β = 90.06°, a = 0.4070 nm, b = 0.4062 nm and c = 0.2870 nm. These parameters are slightly different from those reported by (Saha and Sinha, 2002a, b). Moreover, reports on the same compound revealed crystallization in the pure cubic or monoclinic perovskite structures, but with the presence of residual phases; Table 1 illustrates such results.

The crystallite size was estimated using Scherrer's equation:

$$D = \frac{0,9\lambda}{\beta \cos\theta}$$

Where λ is the X-ray wavelength (1.5406 Å), β is the full-width-at-half-maximum (FWHM) of a characteristic diffraction peak and θ the diffraction angle (the value is calculated from FWHM of the most intense line at the diffraction angle). The estimated value for our sample, heat treated at 900 °C during 8 h, is three time lower than that reported in Ref. (Chao-Yu Chung *et al*., 2005); a special care to the milling process was given to our sample which may explain the low value of the crystallite size.

Characterization by scanning electron microscopy

The microstructure of the BFN powder heat treated at 1100 °C during 8h, revealed by scanning electron microscopy is illustrated in Fig.4. The powder consists of fine particles, with regular morphologiy, and with an average grain size of about770 nm. It also shows a good homogeneity of the sample.

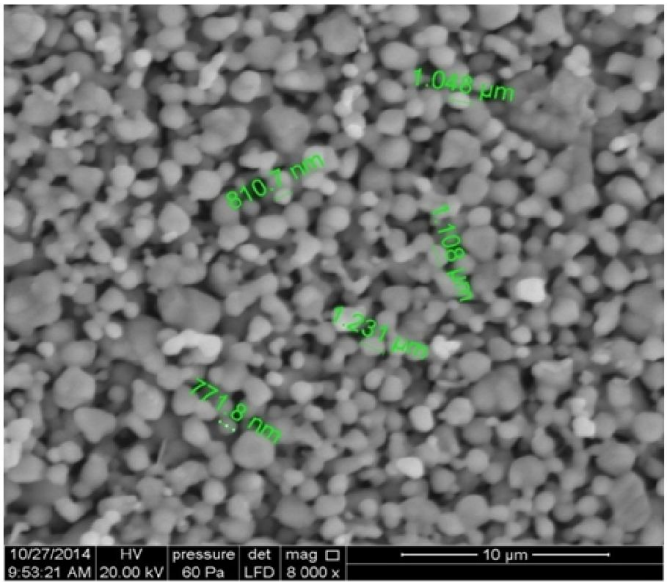

Fig. 4. SEM micrographs of the BFN ceramic sintered at 1100°C for 8h

Dielectric properties

The temperature dependence of the real part of the dielectric permittivity ((ε_r), at different frequencies is shown in Fig.5. It is observed for low frequency values (<10 kHz), and for temperatures inferior or equal to 300°C, the presence of two distinguishable peaks, and for higher frequencies ε_r shows a maximum at a temperature T_m, corresponding to the ferro-to-paraelectric transition, with a strong diffuse character; this maximum shifts to higher temperatures with increasing

Table 1. Comparison of some parameters of the present work related to the as-prepared BFN ceramic with the literature

Method of elaboration	Temperature of calcinations (°C)	Structure	Crystallite size (nm)	Reference
Solid state reaction	1200/4h	Cubic		(M. Ganguly *et al*., 2011)
Solid state reaction	1200 /10h	monoclinic		(Saha and Sinha, 2002)
Molten salt method	900	Cubic	55	(Nattaya *et al*., 2012)
Coprecipitation	850/14h	Monoclinic+ residual phase		(Nipaphat and Rakchart, 2011)
Sol gel	850/5h	Monoclinic+ residual phase	27	(Chao-Yu Chung *et al*., 2005)
Sol gel	900/8h	Monoclinic	9	Present work

frequency which indicates a relaxation process. (Ganguly *et al*., 2011) have observed the presence of two peaks in the thermal behavior of ε_r, in the hole investigated range of frequency (from 10 kHz to 2 MHz). (Saha and Sinha, 2002b) have observed a peak in the thermal variation of the permittivity, for temperatures inferior to 200°C, located at around 172°C (for the frequency 538 Hz). Our results show a maximum of ε_r at 132°C, for the frequency 500 Hz (Table 2). The existence of more than one transition temperature from ferro-to-paraelectric phase may come from the disorder introduced in complex A (B'B'') O_3 perovskites by the presence of two kinds of cations, B' and B'', of different ionic radii, namely Fe^{3+} and Nb^{5+} in the case of $Ba(FeNb)O_3$ perovskites. This disorder, which does not lead to a distortion of the structure, as revealed by XRD analysis, may give rise to composition fluctuation accompanied by different local Curie temperatures (Majumdar *et al*., 2006).

Table 2. Values of the maximum of the permittivity and their corresponding temperatures, for different frequencies

Frequency (kHz)	T_m (°C)	$(\varepsilon_r)_{max}$
0,5	132	4590 (First peak)
1	164	4281 (First peak)
10	238	3553
50	265	2984
100	272	2725
200	276	2486

Dielectric losses of BFN ceramic were measured as a function of temperature up to 300 ◦C at various frequency ranges from 100 kHz to 1MHz, as shown on Fig. 6.Values of loss tangent (tan δ) at room temperature of our ceramics was in the range of 0.1 to 1.2 . The increase of losses with temperature reflects the conducting character of the sample (paraelectric phase). Fig.7 shows dielectric permittivity variations as function of the frequency and for different measuring temperatures. One can observe that the permittivity increases with increasing temperature and the occurrence at high of the frequency, of an anomaly accompanied by a maximum of the permittivity; this maximum shifts to higher frequencies with increasing temperature. Table 3 gathers the observed permittivity values. The existence of such anomaly, at high frequency values, may be attributed to the occurrence of a resonance phenomenon; to our knowledge, existence of such anomaly has not been reported in the literature. Dielectric behavior of the samples was also studied with the help of the modified Uchino's law:

$$\frac{1}{\varepsilon_r} = \frac{1}{\varepsilon_{r\max}}\left[1+\frac{\left(T-T_m\right)^{\gamma}}{2\delta^{\gamma}}\right]$$

Where γ and δ are the relaxor and diffuse parameters, respectively. The samples show a diffuse character of the ferro-to para electric transition (Table 4). A good fitting of the experimental data was performed in Fig.8, and allows determination of the parameters γ and δ. Values of γ are characteristic of a diffuse character. Indeed, γ =1 indicates a normal transition, 1<γ<2 indicates a diffuse character and γ =2 is obtained for relaxor materials.

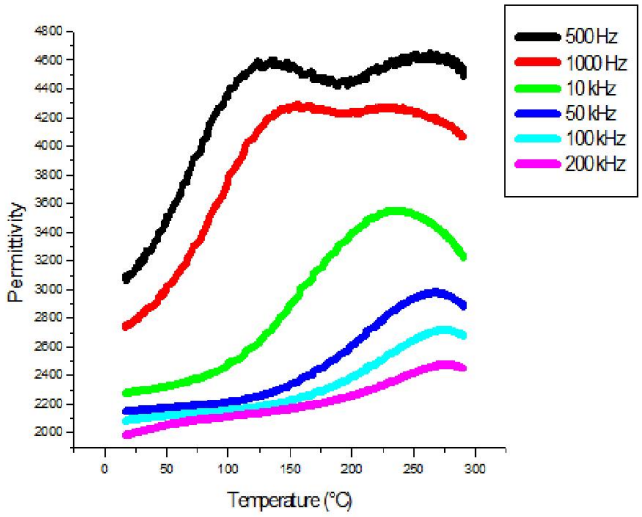

Fig. 5. Thermal variation of the permittivity at different frequencies

Thermal behaviour of the conductivity

Thermal behaviour, for different frequencies, of the conductivity has been studied using the following relation;

$$\sigma = \omega\varepsilon_0\varepsilon'' = \omega\varepsilon_0\varepsilon' \tan\left(\delta\right)$$

The reciprocal temperature dependence of conductivity is shown in Fig.9. With rise in temperature a systematic increase in conductivity is observed which may be due (Eitssayeam *et al*., 2006) to the fact that the concentration of Fe^{2+} ions in the sintered BFN ceramics is highly sensitive to temperature.

Table 3. Values of the maximum of the permittivity and their corresponding temperatures recorded for the anomaly observed at high frequency

Peak position	Corresponding temperature (°C)	Permittivity values (ε))
5,881	ambient	1904
6,011	100	2103
6,061	120	2632
6,077	150	2924
6,093	180	3211
6,093	200	3195
6,093	220	3116
6,044	240	2713
6,028	260	2316
6,011	280	2024

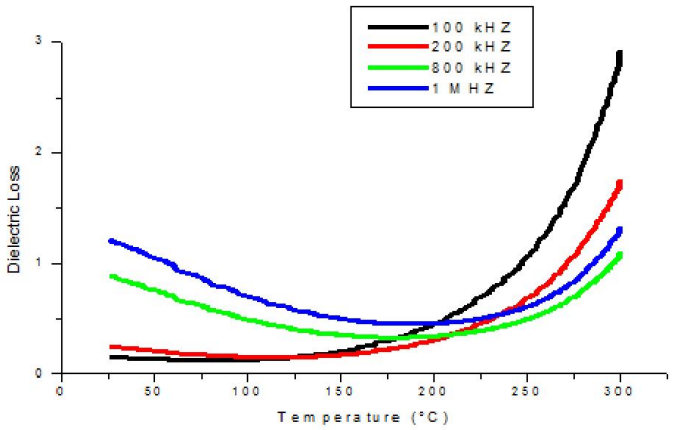

Fig. 6. Temperature dependence of dielectric loss for BFN at various frequencies

This latter shows a diminution of the activation energy as a function of the frequency and are higher than those reported in (Saha and Sinha, 2002b) where the activation value was calculated from Fulcher relation (0.004 eV, a pre-exponential factor of 8.2×10^3 Hz).

To mention that, the activation energy for conduction behavior of oxygen vacancies in the octahedral of any perovskite structure is 1 eV.

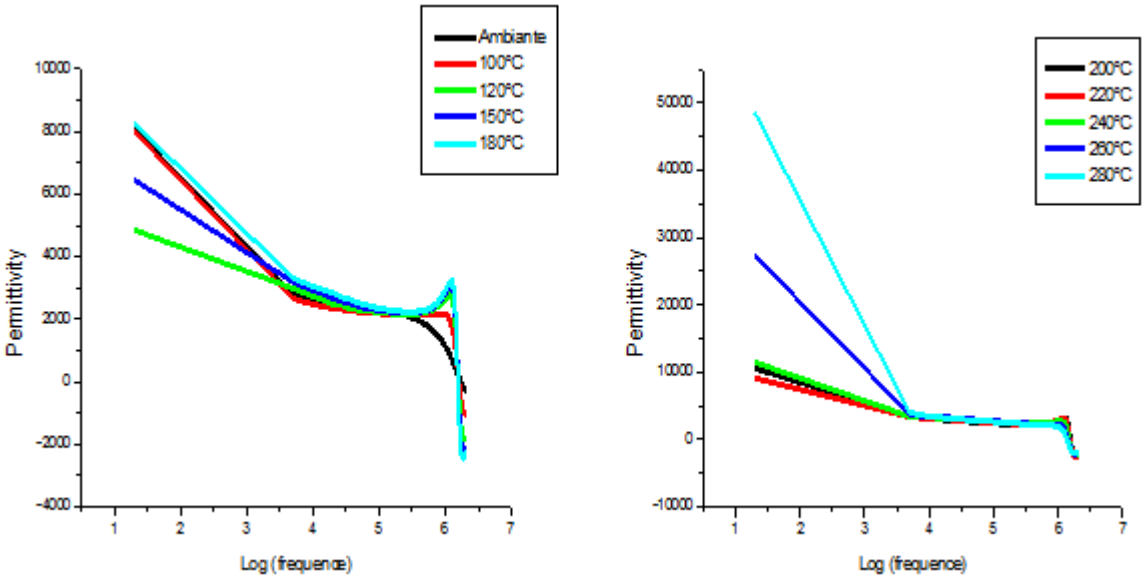

Fig. 7. Frequency dependence of the permittivity for different temperatures

At higher temperatures the long range translational motions of ions contribute to d.c. conductivity. This type of behavior may be explained on the basis of the jump relaxation model (JRM) that considers the conductivity due to successful hops of ions to neighboring vacant sites due to available long time period. It is a already known that the co-existence of Fe^{2+} and Fe^{3+} ions on equivalent crystallographic sites can frequently give rise to an electron hopping type of conduction mechanism. Some kind of vacancies or defects may also have been created as temperature is increased resulting in higher conductivity.

The activation energies of the electric conduction were evaluated using the Arrhenius:

$$\sigma = \sigma_0 e \frac{-E_0}{K_B T}$$

The σ stands for conductivity, σ_0 is the pre-exponential factor, k_B is the Boltzmann factor, T is the absolute temperature and Ea the activation energy which can be calculated from the slope of $\ln\sigma$ as a function of 1/T plot (Fig.10). Values of activation energy are gathered in Table 5.

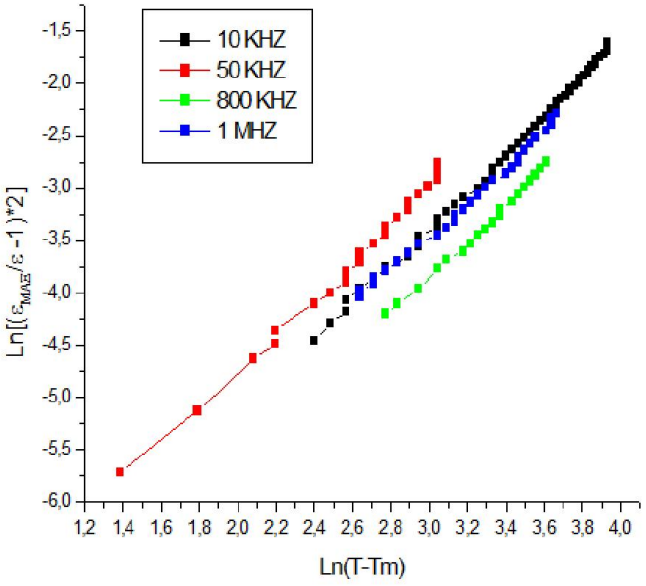

Fig. 8. Plot of $\ln\left(\frac{\varepsilon_m}{\varepsilon}-1\right)$ as a function of $\ln\left(T-T_m\right)$

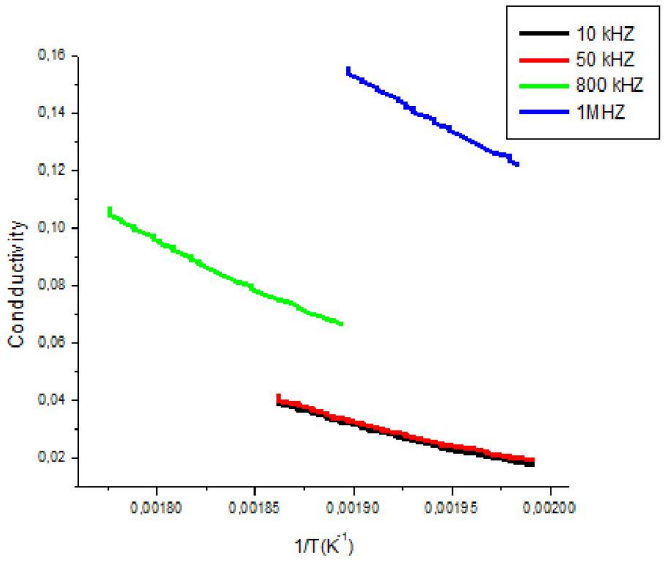

Fig. 9. Temperature dependence of the conductivity for BFN ceramics

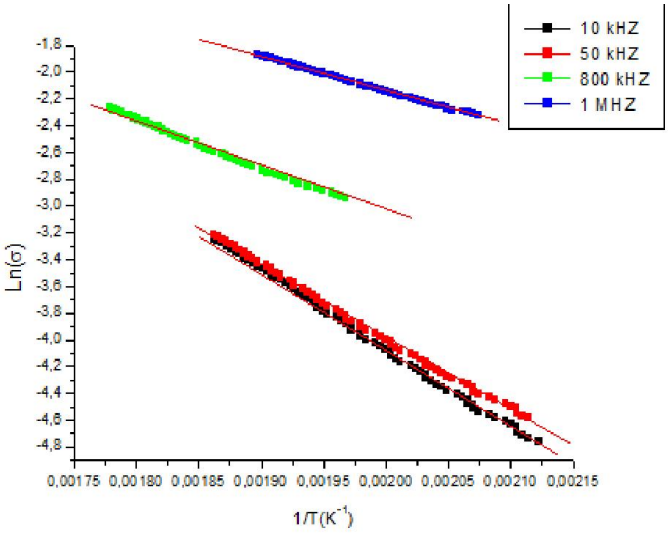

Fig. 10. 'Arrhenius plots for the dc conductivity of BFN for different frequencies

Cole –Cole diagrams

Cole-Cole diagrams for BFN ceramics obtained at different temperatures within the ferroelectric phase are shown in Fig.11. Although the shape of the plots is close to the semicircle, they deviate from a pure Debye relaxation behavior since the semicircles are not centered on the X-axis.

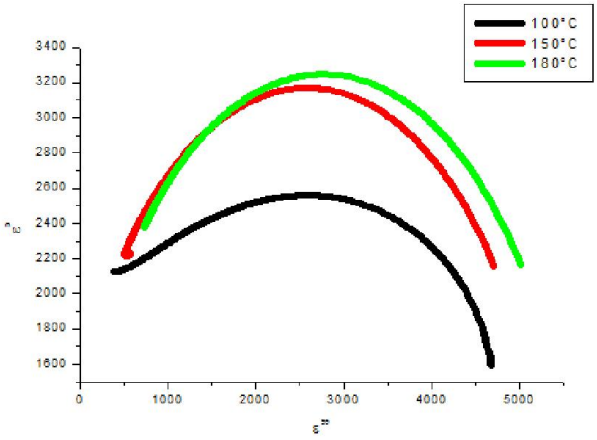

Fig. 11. Cole-Cole diagram BFN

This implies some distribution of relaxation times.

Impedence analysis

Fig.12. shows the variations of the real part, Z', and the imaginary part, Z'', of Z, as functions of frequency and temperature. These two parameters decrease with increasing frequency and temperature. A distinct peak appears in Z''. Decreasing of Z'' with increasing temperature indicate increasing of losses (increasing of conductivity) in the sample. The above mentioned peak shifts towards high frequency region with increasing temperature, indicating that the relaxation process in the material is thermally activated. Moreover, the same evolution of these curves is observed at high frequency pointing out the depletion of space charges (Prabakar and Rao Mallikarjun, 2007).

Piezoelectric properties of BFN

The determination of the piezoelectric parameters is based on the measurements of the resonance and anti-resonance frequencies of the sample.

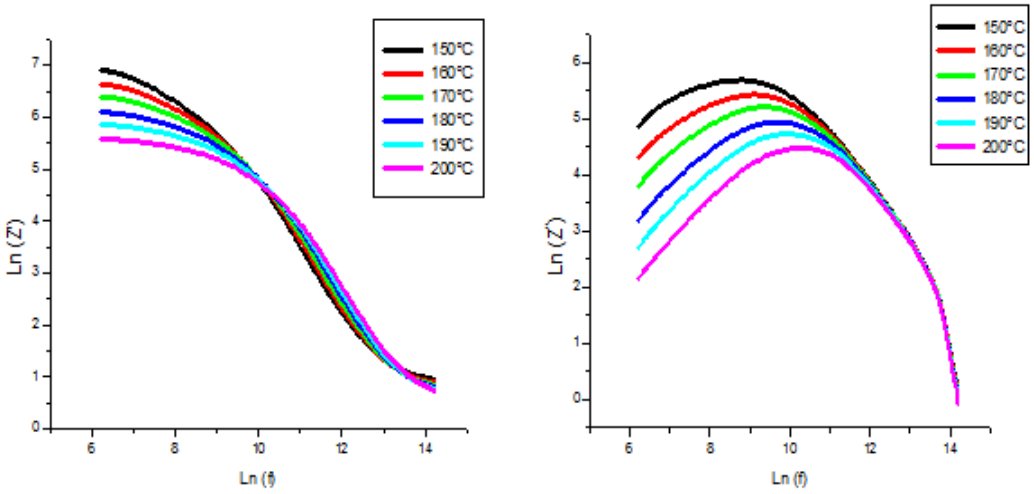

Fig. 12. Variation ln (Z ') and ln (Z' ') as a function of the frequency of BFN

Table 4. γ and δ values for the samples BFN at different frequencies

Fréquency (kHz)	γ	δ
10	1,81	13,24
50	1,79	12,66
800	1,72	14,23
1000	1,62	13,94

(Piezoelectric constant)

$$E = \left[\frac{\pi \Phi f_r}{\eta}\right]^2 * (1-\alpha^{E^2}) * d(N/m^2)$$

(Young's modulus)

$$g_{33} = \frac{d_{33}}{\varepsilon_0 \varepsilon_r}$$

(Voltage constant)

Table 5. Ea values for the samples BFN at different frequencies

Frequencies(kHz)	10	50	400	800	1000
Ea (eV)	0,5167	0,4741	0,3652	0,3114	0,2246

Table 6. Temperature, dielectric constant, Antiresonance frequency, Resonance frequency, Planar coupling coefficient and piezoelectric constant of BFN ceramics sintered at 1100°C for 8h

Temperature (°C)	ε'$_r$	f_a	f_r	k_p	d_{33} (10^{-12} C/N)	g_{33} (10^{14} Vm/N)
100	2103	1947912	1093847	0,92	2,0149	4,4950
120	2799	1926810	1213793	0,87	1,9664	3,3772
180	3260	1882637	1289371	0,82	1,8948	2,9238
220	3087	1853509	1270435	0,81	1,8483	3,0622
260	2316	1791314	1151599	0,85	1,7889	4,3988

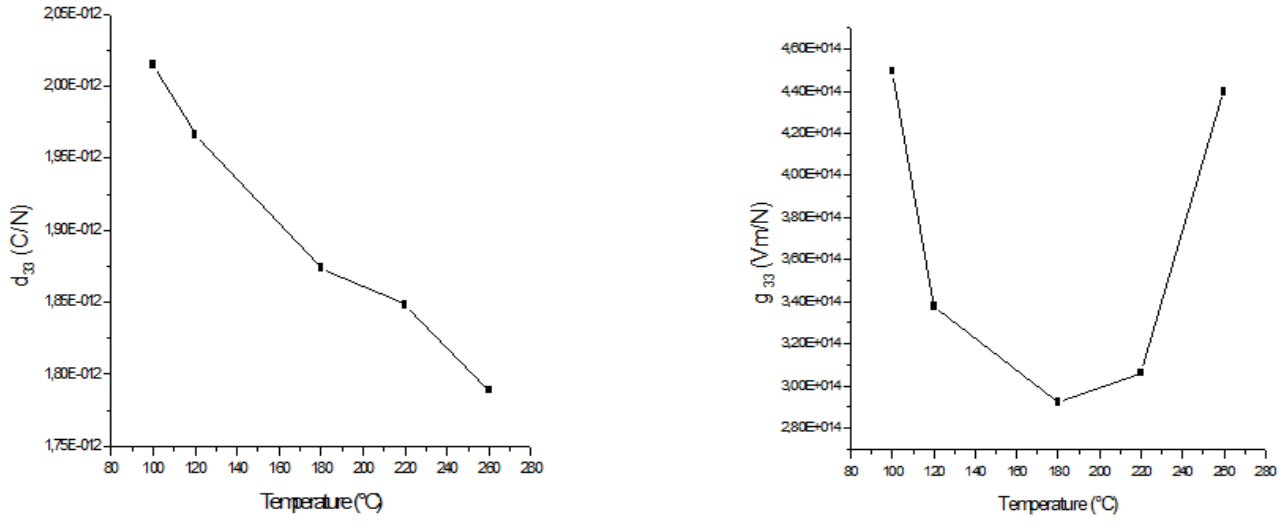

Fig. 13. Variation of the parameter d_{33} and g_{33} as function of the temperature

The latter were calculated using the following formulas:

$$K_p^2 = \frac{\eta^2 - (1-\alpha^{E^2})}{2(1+\alpha^E)} * \frac{f_a^2 - f_r^2}{f_a^2} = \frac{2.51}{2} * \frac{f_a^2 - f_r^2}{f_a^2}$$

(Planar coupling coefficient)

$$d_{33} = K_p \sqrt{\frac{(1-\alpha^E)\varepsilon_r \varepsilon_0}{2E}} (C/N) \ à \ 25°C$$

Where:

Φ: Sample diameter (m).
α^E: Fish coefficient (0.31 for ceramics).
η: The root of the Bessel equation (η=2.05).
D: Density (kg/m^3).
ε_0: Permittivity of the empty = 8.85*10^{-12} (F/m).
ε_r: Relative dielectric permittivity
f_r: Resonance frequency
f_a: Antiresonance frequency

From values of resonance and antiresonance frequencies, values of the parameters d_{33} and g_{33} were determined. Table 6

gathers the values of g_{33} and d_{33} which are temperature dependent. The latter decreases with temperature. The coefficient g_{33} shows the opposite behavior as it is inversely proportional to d_{33} (Fig.13).

Conclusion

BFN samples were successfully elaborated using the sol gel process, and characterized using XRD, MEB and impedance spectroscopy. Results show a crystallization in the pure perovskite phase with monoclinic symmetry, and regular and good morphology. Dielectric measurements revealed a diffuse ferro-to-paraelectric phase with relaxor character; the latter was studied and confirmed by the modified Ushino's law. Values of the temperature of the maximum of the permittivity are lower than those reported in the literature, and we have observed a resonance phenomenon in the frequency dependence of the permittivity, with high values of the latter, which allowed determination of the piezoelectric coefficients. These coefficients are temperature dependent and, in particular, the charge coefficient shows a slight decrease with temperature. Impedance curves showed the presence of depressed semicircles in Cole-Cole diagrams signature of a distribution of relaxation times; the corresponding behavior deviates from pure Debye relaxation.

Acknowledgements

The authors would like to thank Profs. F. Abdi, T. Lamcharfi (FST, Fès, Morocco) for their technical support and fruitful discussions.

REFERENCES

Chao-Yu Chung, Yen-Hwei Chang, Guo-Ju Chen, Yin-Lai Chai, Preparation, structure and ferroelectric properties of Ba (Fe0.5Nb0.5) O_3 powders by sol–gel method, *Journal of Crystal Growth,* 284 (2005) 100–107.

Eitssayeam, S., Intatha, U., Pengpat, K. and Tunkasiri, T. 2006. Preparation and characterization of barium iron niobate $BaFe0.5Nb0.5O_3$ ceramics, *Current Applied Physics,* 6, 316–318.

Homes, C.C., Vogt, T., Shaprio, S.M., Wakimoto, S., Subramanian, M.A. and Ramirez, A.P. 2003. Charge transfer in the high dielectric constant materials $CaCu_3Ti_4O_{12}$ and $CdCu_3Ti_4O_{12}$, *Physical Review*, B 67, 092106-1–092106-4.

Limame, K., Sayouri, S., El Ghazouali, A., Hajji, L., Lamcharfi, T., Jaber, B. and Housni, A. 2008. Diffuse Phase Transition, Relaxor Behavior and Anomalies in (Pb, La)TiO_3 Ceramics, *Ferroelectrics,* 371, 68.

Majumdar, S.B. Bhattacharya, D. Katiyar, R.S. Manivannan, A. Dutta, P. and Seehra, M.S. 2006. Dielectric and Magnetic roperties of Sol-Gel Derived Pb(Fe0.5Nb0.5)O3 Ceramics, *J. Appl. Phys.,* 99, 024108.

Nattaya Tawichai, Waraporn Sittiyot, Sukum Eitssayeama, Kamonpan Pengpat, n Tawee Tunkasiri, Gobwute Rujijanagul, 2012. Preparation and dielectric properties of barium iron niobate by molten-salt synthesis, Ceramics International 38S, S121–S124.

Nipaphat Charoenthai and Rakchart Traiphol, Progress in the synthesis of Ba (Fe0.5Nb0.5) O_3 ceramics: A versatile co-precipitation method, *Journal of Ceramic Processing Research,* 12 (2011) 191~194.

Prabakar, K. 2007. Rao Mallikarjun, Complex impedance spectroscopy studies on fatigued soft and hard PZT ceramics, *J. Alloys and Compounds,* 437, 302.

Raevski, I.P., Prosandeev, S.A. and Osipenko, I.A. 1996. Nature of the forbidden gap in insulating $AB_xB'_{1-x}O_3$ crystals, *Phys. Stat. Sol.,* (b) 198, 695–705.

Raevski, I.P., Prosandeev, S.A., Bogatin, A.S., Malitskay, M.A. and Jastrabik, L. 2003. High dielectric permittivity in $AFe_{1/2}B_{1/2}$ O_3 nonferroelectric perovskite ceramics (A = Ba, Sr, Ca; B = Nb, Ta, Sb), *Journal of Applied Physics,* 93, 4130–4136.

Rama, N. Philipp, J.B., Opel, M., Chandrasekaran, K., Gross, R. and Ramachandra Rao, M.S. 2004. Preparation, electrical conductivity, and magnetic susceptibility of (Ba_{1-X} Bi_x) (Mn0.5 + x/2Nb 0.5 - X/2) O_3, *Journal of Applied Physics*, 95, 7528–7530.

Saha, S. and Sinha, T.P. 2002. Low-temperature scaling behavior of $BaFe0.5Nb0.5O_3$, Physical Review B 65, a 134103–134111.

Saha, S. and Sinha, T.P. 2002. Structural and dielectric studies of $BaFe0.5Nb0.5O_3$, *Journal of Physics: Condensed Matter*, 14, b 249–258.

Subramanian, M.A., Li, D., Duan, N., Reisner, B.A. and Sleight, A.W. 2000. High dielectric constant in ACu3Ti4O12 and $ACu_3Ti_3FeO_{12}$ phases, *Journal of Solid State Chemistry,* 151, 323–325.

Tezuka, K., Henmi, K. and Hinatsu, Y. 2000. Magnetic susceptibility and Mossbauer spectra of perovskites A_2-$FeNbO_6$ (A = Sr, Ba), *Journal of Solid State Chemistry*, 154 (2000) 591–597.

Yokosuka, M. 1995. Dielectric dispersion of the complex perovskite oxide $Ba(Fe_{1/2}$ $Nb_{1/2})O_3$ at low frequencies, *Japanese Journal of Applied Physics,* 34,5338–5340.

****